Biomimetic Sensors

DOI: 10.1002/ange.201305368

Coupling Biocatalysis with Molecular Imprinting in a Biomimetic Sensor**

*Aysu Yarman and Frieder W. Scheller**

Fully synthetic molecularly imprinted polymers (MIPs) are expected to substitute antibodies in bioanalysis and chromatography in the future.[1–3] In addition to binding MIPs, catalytically active MIPs have been developed (see the Supporting Information) for application in sensors and syntheses.[4,5] So far, however, the affinity and catalytic activity of MIPs have in general been lower than those of their biological counterparts. Hybrids composed of a biocatalyst and a MIP may combine the advantages of both components. This combination should improve selectivity in sensors that operate on the basis of either a "group-specific" enzyme or a binding MIP. However, the harsh conditions of MIP preparation have not previously been compatible with the stability of enzymes.

Herein we describe the first combination of a molecularly imprinted electropolymer with a biocatalyst in a catalytic biomimetic sensor. We applied both highly active horseradish peroxidase (HRP) and the "minienzyme" microperoxidase-11 (MP-11). The peroxide-dependent substrate conversion takes place in a layer on top of a product-imprinted electropolymer on the indicator electrode (Figure 1). The hierarchical architecture enables the optimization of both parts prior to their combination. This arrangement resulted in the elimination of interfering signals for ascorbic acid (AA) and uric acid (UA) both in a phosphate buffer and in diluted serum samples.

For HRP and MP-11, a whole spectrum of peroxide-dependent reactions has been described.[6,7] Notably, MP-11 also possesses P450-like activity and has been used to oxidize hydrophobic substances, including drugs in organic solvents; therefore, it is an attractive catalyst for biomimetic sensors. In this study, we extended the spectrum of MP-11-based sensors to the N-demethylation exemplified for the analgesic drug aminopyrine (AP). AP is metabolized by NADPH-dependent catalysis by liver cytochromes P450 to formaldehyde and aminoantipyrine (AAP), which is devoid of the two methyl groups at N4 (Scheme 1; NADPH is the reduced form of nicotinamide adenine dinucleotide phosphate). The same demethylated products are also formed in the HRP-catalyzed reaction.[8]

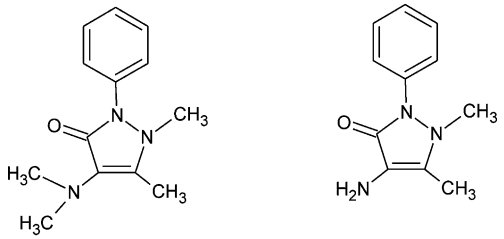

Scheme 1. Structures of the analyte AP and the template AAP.

In the HRP- and MP-11-catalyzed peroxide-dependent oxidation of AP, a purple-colored intermediate with an absorption maximum at 550 nm was formed. The radical intermediate derived from AP (but not AAP) generated at the MP-11-modified glassy carbon electrode (GCE) a cathodic current at 0 mV which was linearly dependent on the AP concentration from 1 to 5 μM with a linear correlation coefficient of 0.9871. The limit of detection (LOD) was determined to be 584 nM (signal-to-noise ratio, S/N = 3). The signal obtained for the conversion of AP (1 μM) was found to be almost eightfold lower than the respective signal for the optimal substrate *p*-aminophenol. Clearly, the indication of an intermediate instead of a final product is the reason for the lower sensitivity. With an HRP-modified GCE, the linear range was extended to 90 μM with an LOD of 821.8 nM (S/N = 3).

Since HRP and MP-11 catalyze the peroxide-dependent conversion of a very broad range of substrates, the sensors generate an "overall signal", which sums up the contribution of all convertible substances. To narrow down the spectrum of substances involved in the measurement signal, we covered the electrode with a product-imprinted electropolymer. As previously described by Weetall and Rogers,[9] we applied a mixture of *o*-phenylenediamine (*o*-PD) and resorcinol (Res) as functional monomers and AAP as the target to form recognition sites in a molecularly imprinted electropolymer cover layer.

AAP alone showed an irreversible oxidation peak at 519 mV at the bare GCE (see Figure S1 in the Supporting Information). Oligomers are formed following the electro-

[*] Dr. A. Yarman, Prof. Dr. F. W. Scheller
Fraunhofer Institute for Biomedical Engineering
Am Mühlenberg 13, 14476 Potsdam (Germany)
and
Institute of Biochemistry and Biology, University of Potsdam
Karl-Liebknecht-Strasse 24–25, 14476 Potsdam (Germany)
E-mail: fschell@uni-potsdam.de

[**] We thank Alexander Christmann for the AFM investigations and the BMBF (0311993) of Germany for financial support. This research forms part of UniCat, a Cluster of Excellence in the field of catalysis that is coordinated by the Technical University of Berlin and supported financially by the Deutsche Forschungsgemeinschaft (DFG) within the framework of the German Excellence Initiative (EXC 314).

Supporting information for this article is available on the WWW under http://dx.doi.org/10.1002/anie.201305368.

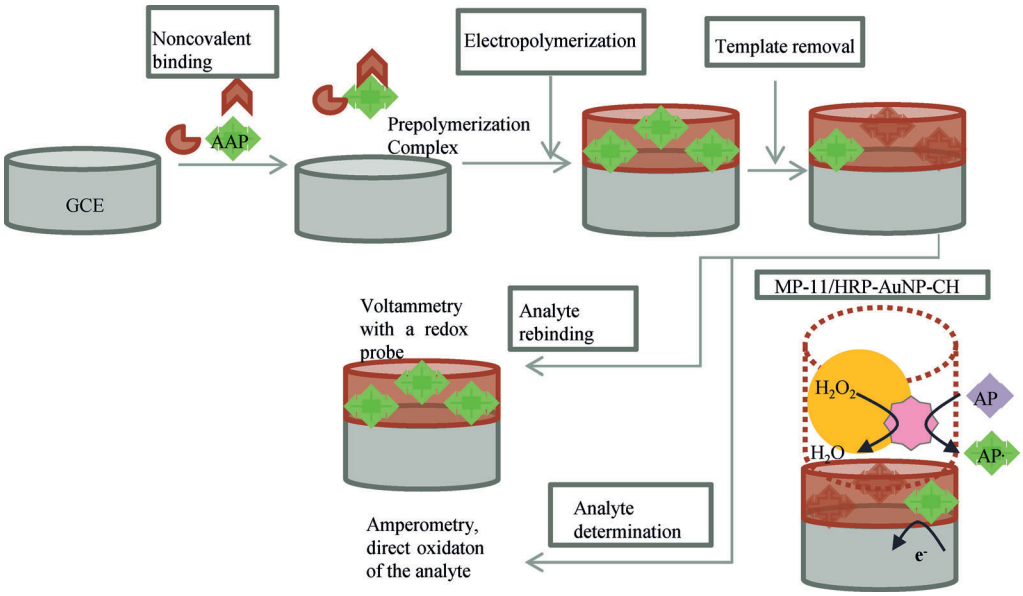

Figure 1. Schematic representation of sensor preparation and the measurement process.

chemical generation of radicals.[10] Cycling of the electrode potential between 0 and 0.8 V in the *o*-PD/Res mixture in the absence (preparation of the nonimprinted polymer, NIP) or in the presence of AAP (preparation of the MIP) led to similar voltammograms (see Figure S1). The oxidation current decreased during the following sweeps and approached zero after 20 sweeps; this behavior is typical of a nonconducting polymeric film.

We used ferricyanide as a redox probe to characterize the permeability of the layer after electropolymerization. With the MIP- and NIP-modified GCEs, there was almost complete suppression of the ferricyanide peaks after film formation. Incubation of the MIP-covered electrode in aqueous sodium hydroxide resulted in the removal of the template, as revealed by the detection of AAP and its oligomers by mass spectroscopy in the eluate and a marked increase in the ferricyanide signal. The signal for ferricyanide was suppressed again after interaction of the MIP layer with AAP (Figure 2). Clearly, upon template removal, pores to the electrode were formed that contained "imprints" of AAP and its oligomers. Treatment of the NIP with NaOH led only to a small increase in the permeability of the redox marker, and interaction with AAP had a negligible effect. This behavior indicated the absence of an imprinting effect for the NIP.

Unlike in some previously reported studies,[15–18] the layer was less dense at higher template concentrations. When electropolymerization was performed at pH 7, the template could be removed, but rebinding at pH 7 was not observed.

After optimization of the electropolymerization conditions, such as the template concentration, template-removal time, and pH value, we studied the amperometric response for the rebinding of AAP. AAP is electroactive in the anodic potential region, and the amperometric response of both the bare and the imprinted glassy carbon electrode at 500 mV was linearly dependent on the AAP concentration. For the imprinted electrode, the current increased linearly between

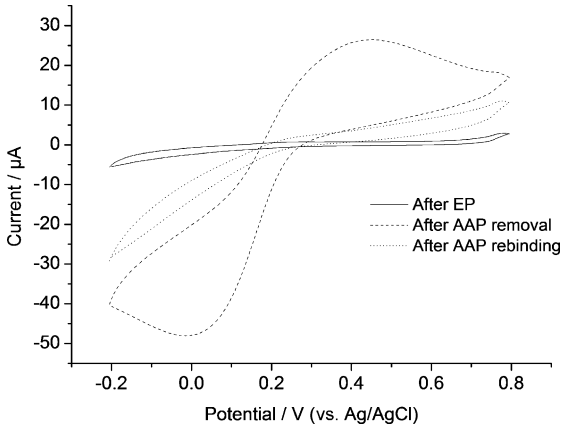

Figure 2. Overlay of cyclic voltammograms recorded for the MIP electrode after electropolymerization (solid line), after AAP removal (dashed line), and after AAP rebinding (dotted line) in an aqueous solution of KCl (100 mM) and ferricyanide (10 mM) at a scan rate of 50 $mV s^{-1}$.

10 and 100 µM with a regression coefficient of 0.9963 (see Figure S2). The limit of detection was determined to be 141 nM (S/N = 3). At higher concentrations, no steady state was observed, probably as a result of the binding of AAP to the cavities and the formation of an oligomeric AAP species.

At +500 mV, the bare electrode and the sensor covered with the AAP-MIP showed current signals for AP that were almost 25% smaller than those for AAP. This result shows that the AAP-MIP does not differentiate the two substances, which differ only in two methyl groups. The polymerization of AAP during the formation of the MIP may lead to "imprints" in which the N4 position is hidden between two monomer units.[10] Therefore, the AAP-MIP indicates the total amount of AAP and AP in mixtures of these substances.

The signal at +500 mV for AAP was not influenced by the presence of a tenfold excess of the potentially interfering

substances ascorbic acid (AA), uric acid (UA), and caffeine (see Figure S3). The amperometric response of each interfering substance at the bare electrode, the AAP-imprinted electrode, and the nonimprinted electrode was compared with that observed for AAP (Figure 3). Since ascorbic acid and

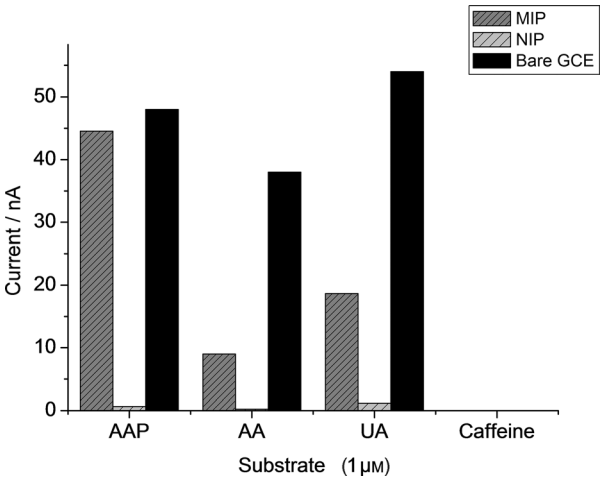

Figure 3. Comparison of the signals of the template and interfering substances on bare, nonimprinted, and AAP-imprinted GCEs.

uric acid are electroactive, they cause an anodic current at 500 mV. In contrast, caffeine is not electroactive at this potential. On the bare GCE, almost equal responses were observed for AAP and the potentially interfering substances. However, the highest response with the AAP-imprinted electrode was observed for the template AAP itself. The imprinting effect, which should be based on the generation of specific binding sites, is illustrated in Figure 3, which shows pronounced suppression of the signals for AA and UA in relation to the signal of the target AAP with respect to the bare electrode. Thus, the AAP-MIP shows preferential permeability for AAP as compared with interfering substances.

We compared the electrochemical signals at + 500 mV of AAP, AA, and UA for the AAP-imprinted MIP with those of a desmethyltamoxifen MIP (dm-TAM-MIP). In these experiments, we used the same matrix (*o*-PD/Res) in both MIPs to demonstrate the "contribution of the imprinting". Whereas for the AAP-MIP, the current for UA was 4.96 times smaller than that for AAP, for the dm-TAM-MIP, the current for UA was only 1.3 times smaller than that for AAP. The currents observed for AA and AAP differed by a factor of 2.39 with the AAP-MIP and by a factor of 1.5 with the dm-TAM-MIP. The considerably smaller difference between the AAP and UA signals with the dm-TAM-MIP (which has no binding sites for AAP) is a further indication of imprinting of the electropolymer by the target.

The surface morphology of the MIP-covered electrodes was visualized by atomic force microscopy (AFM). After incubation in aqueous NaOH, the roughness of the NIP and MIP as reflected by root-mean-square values of 1.11 and 1.18 nm was very close to that of the bare electrode (0.90 nm). Furthermore, the surface of the MIP layer showed features in

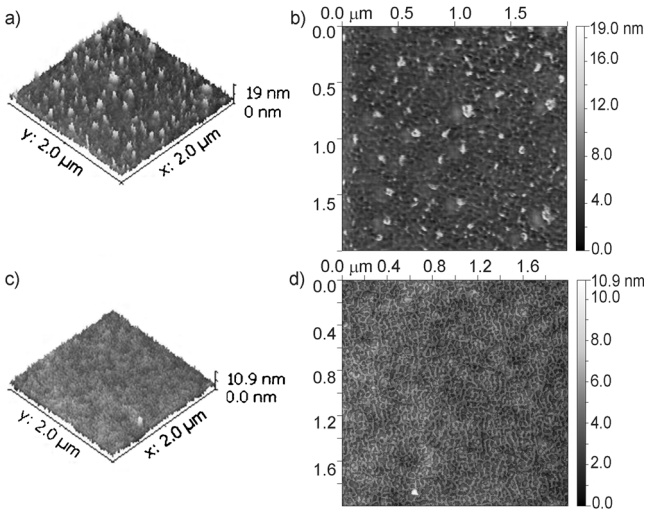

Figure 4. a,c) 3D and b,d) 2D AFM images of an AAP-imprinted electrode after electropolymerization (a,b) and after AAP removal with 0.1 M aqueous NaOH (c,d).

the range of 20 nm in diameter which extended up to the electrode surface (Figure 4). Similar porous structures have been observed for electropolymers imprinted with a nonapeptide, L-glutamate, and folic acid.[12–14] It is generally assumed that pores in MIPs for low-molecular-weight substances have a larger diameter than the target molecule[11] and that the majority of "binding pockets" are at the inner walls of the pores.

At lower template concentrations, the template could not be removed effectively, as indicated by very small signals for ferricyanide and for AAP after treatment with NaOH. The AFM image of the respective MIP was very similar to that of the NIP and devoid of pore structures (see Figure S4).

In the case of the nonimprinted electrode, negligible signals for AAP were always observed. The imprinting factor was calculated to be 6.67 on the basis of the equation: imprinting factor = (signal of MIP)/(signal of NIP). The imprinting factor and the selectivity coefficients[13,18,20] were comparable with those of surface-imprinted MIPs. For bulk imprints, better values have been reported previously in a few cases, because a large number of "separation plates" results in more efficient separation.[21] However, this advantage comes at the expense of considerably longer response times.[22]

As an example a MIP for AP was prepared by thermal bulk polymerization with methacrylic acid as the functional polymer. A solution of the polymer in tetrahydrofuran was dropped onto the electrode of a quartz crystal microbalance. The MIP sensor responded in the lower micromolar range and showed twofold to fourfold higher sensitivity as compared with the nonimprinted polymer. The intensity of signals for competing substances, for example, caffeine and paracetamol (at 1 μM), were around 40% of the value observed for the target. The measuring cycle extends over 60 min, including a response time of 20 min.[22]

Our MIP sensor responded in real time to both an increase in the concentration of the target analyte and dilution by the measurement buffer and reached the steady

state within 5 s (see Figures S2, S5, and S6). It required regeneration only after a series of measurements. Up to a concentration of 100 μM of AAP, the sensor was regenerated by incubation in the background buffer. At higher concentrations, the electrode was partially blocked by electropolymerized AAP and regeneration required incubation in NaOH. The fast response and also the fast removal of the template are remarkable advantages as compared with the harsh washing conditions and long response times typically described for MIPs.[19]

The AAP-imprinted sensor was also evaluated in diluted serum (1:40) spiked with physiological concentrations of AAP and the interfering substances (see Figure S6). Only at elevated concentrations of AA after vitamin dosage (an AA concentration above 500 μM) or in hyperuricemic patients (an UA concentration higher than 400 μM) would the signals for AAP (1 mM) be falsely increased by more than 5–10%.

To completely eliminate the contribution of electrochemically interfering substances, we spatially integrated enzymatic analyte conversion by MP-11 or HRP and filtering by a product-imprinted electropolymer layer: The biocatalysts were placed in a layer on top of the product-imprinted electropolymer on the indicator electrode. On the stepwise addition of AP, the cathodic current at 0 mV of the MP-11–MIP/GCE increased linearly between 1 and 13 μM with a regression coefficient of 0.9957 and reached saturation at higher concentrations. In the case of the HRP–MIP/GCE, the linear range was extended to 110 μM, and the sensitivity was almost twice as high (see Table S1 in the Supporting Information). Furthermore, the effect of the interfering substances AA and UA was studied with MP-11–MIP/GCE and HRP–MIP/GCE. UA gave no response, since it is not electroactive at 0 mV. The contribution of AA was also completely suppressed by the action of the MIP layer and oxidation with peroxide (Figure 5). The peroxide-dependent oxidation catalyzed by MP-11 or HRP leads only with AP but not with AAP to a steady-state current signal at 0 mV. Therefore, the combined MP-11–MIP sensor indicates only AP (also in the presence of AAP) and prevents interference by AA or UA. Our approach competes very well with previously described MIP sensors with respect to the analytical parameters, including the lower limit of detection, the complete elimination of cross-reactivity with AA, and in particular the response time of 10–15 s (see Table S1).[23–26]

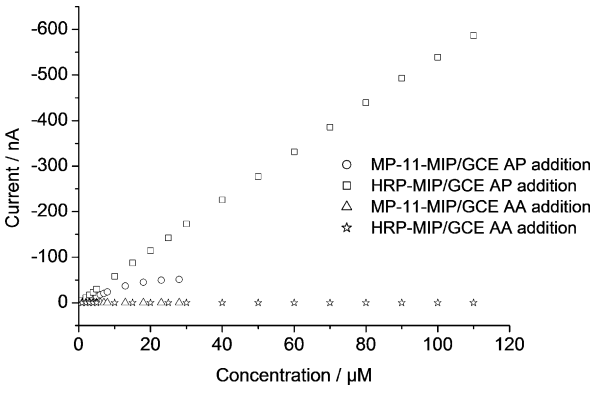

Figure 5. Current–concentration curves for MP-11–MIP/GCE and HRP–MIP/GCE for the stepwise addition of AP or AA.

The formation of the "sandwich structure" is straightforward: After in situ formation of the molecularly imprinted layer on the surface of the electrode, the biocompatible chitosan layer, which contains the biocatalyst, is cast on the MIP layer. This approach of combining a MIP with a thin layer of a biocatalyst is generally applicable for the suppression of electrochemical interference. On the other hand, the application of a charged cover membrane, for example, nafion, or an enzyme-containing "anti-interference layer"[27] is only effective for selected substances.

An advantage of the new hierarchical structure is the separation of MIP formation by electropolymerization and immobilization of the catalyst. In this way, it was possible for the first time to integrate an enzyme—HRP—with an MIP layer in a sensor configuration. This combination has the potential to be transferred to other enzymes, for example, P450, and could thus enable the detection of clinically important analytes.

Experimental Section

AAP-imprinted GCEs were prepared in an *o*-PD (5 mM)/resorcinol (5 mM) mixture (in 100 mM acetate buffer, pH 5.2) containing AAP (0.1–10 mM) by cyclic voltammetry by sweeping between 0 and 0.8 V (20 scans) at a scan rate of 50 $mV\,s^{-1}$. The same procedure was applied with desmethyltamoxifen (0.4 mM) for the preparation of a dm-TAM-imprinted polymer. Nonimprinted electrodes were prepared in a similar way in the absence of a template. Template molecules were removed by incubation in a 100 mM aqueous solution of NaOH overnight.

MP-11–MIP/GCEs and HRP–MIP/GCEs were prepared in two steps: First, electropolymerization was performed as described above, and template molecules were removed. A 1:1 (v/v) mixture of MP-11 or HRP and chitosan capped gold nanoparticles (AuNP-CH) was then dropped onto the electrode and dried overnight in a refrigerator at 4 °C, as described previously.[7b]

Amperometric measurements were performed under aerobic conditions in a phosphate buffer (10 mM, pH 7). Working potentials of 500 and 0 mV were applied for the direct oxidation and for the combination of the enzyme with the MIP, respectively.

Received: June 21, 2013
Published online: September 5, 2013

Keywords: biomimetic sensors · electropolymers · enzymes · hierarchical structures · molecularly imprinted polymers

[1] K. Haupt, K. Mosbach, *Trends Biotechnol.* **1998**, *16*, 468–475.
[2] O. Hayden, P. A. Lieberzeit, D. Blaas, F. L. Dickert, *Adv. Funct. Mater.* **2006**, *16*, 1269–1278.
[3] M. Frasconi, R. Tel-Vered, M. Riskin, I. Willner, *Anal. Chem.* **2010**, *82*, 2512–2519.
[4] G. Wulff, *Angew. Chem.* **1995**, *107*, 1958–1979; *Angew. Chem. Int. Ed. Engl.* **1995**, *34*, 1812–1832.
[5] A. Servant, K. Haupt, M. Resmini, *Chem. Eur. J.* **2011**, *17*, 11052–11059.
[6] W. Y. Jeng, Y. H. Tsai, W. J. Chuang, *J. Pept. Res.* **2004**, *64*, 104–109.
[7] a) A. Yarman, T. Nagel, N. Gajovic-Eichelmann, A. Fischer, U. Wollenberger, F. W. Scheller, *Electroanalysis* **2011**, *23*, 611–618;

b) A. Yarman, A. Badalyan, N. Gajovic-Eichelmann, U. Wollenberger, F. W. Scheller, *Biosens. Bioelectron.* **2011**, *30*, 320 – 323; c) A. Yarman, B. Neumann, M. Bosserdt, N. Gajovic-Eichelmann, F. W. Scheller, *Biosensors* **2012**, *2*, 189 – 204.

[8] B. W. Griffin, P. L. Ting, *Biochemistry* **1978**, *17*, 2206 – 2211.

[9] a) H. H. Weetall, K. R. Rogers, *Talanta* **2004**, *62*, 329 – 335; b) H. H. Weetall, D. W. Hatchett, K. R. Rogers, *Electroanalysis* **2005**, *17*, 1789 – 1794.

[10] H. Sayo, M. Masui, *J. Chem. Soc. Perkin Trans. 2* **1973**, 1640 – 1645.

[11] a) S. C. Zimmerman, N. G. Lemcoff, *Chem. Commun.* **2004**, 5 – 14; b) "Molecular Imprinting": K. Haupt, A. V. Linares, M. Bompart, B. Tse Sum Bui in *Topics in Current Chemistry*, *Vol. 325* (Ed.: K. Haupt), Springer, New York, **2012**, pp. 1 – 28; c) S. A. Piletsky, T. L. Panasyuk, E. V. Plisetskaya, I. A. Nicholls, M. Ulbricht, *J. Membr. Sci.* **1999**, *157*, 263 – 278.

[12] D. Dechtrirat, K. J. Jetzschmann, W. F. M. Stöcklein, F. W. Scheller, N. Gajovic-Eichelmann, *Adv. Funct. Mater.* **2012**, *22*, 5231 – 5237.

[13] R. Ouyang, J. Lei, H. Ju, Y. Xue, *Adv. Funct. Mater.* **2007**, *17*, 3223 – 3230.

[14] D. C. Apodaca, R. B. Pernites, R. R. Ponnapati, F. R. Del Mundo, R. C. Advincula, *ACS Appl. Mater. Interfaces* **2011**, *3*, 191 – 203.

[15] C. Malitesta, I. Losito, P. G. Zambonin, *Anal. Chem.* **1999**, *71*, 1366 – 1370.

[16] J. Kang, H. Zhang, Z. Wang, G. Wu, X. Lu, *Polym.-Plast. Technol.* **2009**, *48*, 639 – 645.

[17] X. Kan, T. Liu, H. Zhou, C. Li, B. Fang, *Microchim. Acta* **2010**, *171*, 423 – 429.

[18] W. Song, Y. Chen, J. Xu, X.-R. Yang, D.-B. Tian, *J. Solid State Electrochem.* **2010**, *14*, 1909 – 1914.

[19] a) J. P. Li, F. Y. Jiang, X. P. Wei, *Anal. Chem.* **2010**, *82*, 6074 – 6078; b) M. Blanco-López, M.-J. Lobo-Castañón, A. J. Miranda-Ordieres, P. Tuñón-Blanco, *Anal. Bioanal. Biochem.* **2003**, *377*, 257 – 261; c) X. Kan, T. Liu, H. Zhou, C. Li, B. Fang, *Microchim. Acta* **2010**, *171*, 423 – 429.

[20] P. S. Sharma, A. Pietrzyk-Le, F. D'Souza, W. Kutner, *Anal. Bioanal. Chem.* **2012**, *402*, 3177 – 3204.

[21] L. R. Sartori, W. de Jesus Rodrigues Santos, L. T. Kubota, M. G. Segatelli, C. R. T. Tarley, *Mater. Sci. Eng. C* **2011**, *31*, 114 – 119.

[22] Y. Tan, L. Nie, S. Yao, *Analyst* **2001**, *126*, 664 – 668.

[23] F. Berti, S. Todros, D. Lakshmi, M. J. Whitcombe, I. Chianella, M. Ferroni, S. A. Piletsky, A. P. F. Turner, G. Marrazza, *Biosens. Bioelectron.* **2010**, *26*, 497 – 503.

[24] D. Antuña-Jiménez, M. C. Blanco López, A. J. Miranda Ordieres, P. Tuñón Blanco, M. J. Lobo Castañón, *14th International Conference on Electroanalysis*, Slovenia, **2012**.

[25] J. R. M. Neto, W. de Jesus Rodrigues Santos, P. R. Lima, S. M. C. N. Tanaka, A. A. Tanaka, L. T. Kubota, *Sens. Actuators B* **2011**, *152*, 220 – 225.

[26] K. Sode, S. Ohta, Y. Yanai, T. Yamazaki, *Biosens. Bioelectron.* **2003**, *18*, 1485 – 1490.

[27] a) G. Nagy, M. E. Rice, R. N. Adams, *Life Sci.* **1982**, *31*, 2611 – 2616; b) U. Wollenberger, F. Scheller, D. Pfeiffer, V. A. Bogdanovskaya, M. R. Tarasevich, G. Hanke, *Anal. Chim. Acta* **1986**, *187*, 39 – 45.

